

An Automated Change Detection Approach for Mine Recognition Using Sidescan Sonar Data

Shuang Wei, Henry Leung
Department of Electrical and Computer Engineering
University of Calgary
Calgary, AB, CANADA
swei@ucalgary.ca, leungh@ucalgary.ca

Vincent Myers
Defence R&D Canada
Dartmouth, Nova Scotia,
CANADA
vincent.myers@drdc-rddc.gc.ca

Abstract—This paper presents a new automated approach for the mine detection and classification (MDC) problem based on change detection techniques using sidescan sonar images. Adopting change detection techniques benefits this approach to recognize mine targets without training data or prior assumption required in traditional detection methods. In this approach, post-classification comparison is designed to detect the changes and the statistical information of pixel distribution is employed for change decision analysis. Specifically, because of the special characteristics of shadows in sonar images, shape and coarseness features are taken into account and play an important role in this method. This approach was successfully applied to two sets of bi-temporal sidescan sonar images and the results are presented in this paper. The results prove the applicability of this approach for mine detection.

Index Terms—Change detection, Mine detection and classification, Sidescan sonar, Post-classification comparison, Coarseness

I. INTRODUCTION

With the development of sidescan sonar techniques, more and more high resolution images of the seafloor can be obtained, the analysis of which is essential for mine countermeasures (MCM) in the civilian and military applications. Nevertheless, it is challenging to exactly recognize the target mines in the sonar images due to a high density of interfering debris on the seafloor and large environmental variations in the sidescan images. Additionally, certain unpredictable objects similar to the target mines on the seafloor inevitably create a prohibitive number of false alarms.

Nowadays, most approaches for automated MCM using sidescan sonar data take up MDC process to replace the traditional manual operations. In the MDC process, all mine-like objects (MLOs) are detected first, and mine targets and not-mine objects are then classified among the MLOs. Traditionally, approaches [1][2][3] based on supervised classification techniques were employed that required a large amount of training data which should have the similar characteristics as the testing data. Later, an unsupervised approach for detection was proposed in [4] to avoid the limitation of training data, using available a priori spatial information on the appearance of mine signatures and the a priori information on the relationship between the highlight and shadow of objects. Besides this, [5] utilized the ideal shadow information calculated by line-of-sight principle of mine targets with special shapes

(i.e., cylinder, sphere and cone) for classification. Thus, it can be observed that all the approaches addressing the MDC problem using a single image require additional supporting information to assist the image analysis (i.e. training data or model assumptions). However, training data for all the mine targets can not always be obtained easily and some model assumptions lack the strong theoretical basis. Meanwhile, route survey operations provide an opportunity to reserve a database of historical sidescan sonar data. Therefore, this paper suggests applying change detection techniques to deal with the MDC problem using two sidescan sonar images taken in different dates to avoid the need for any training data or assumptions constraints.

Change detection techniques have been widely used for remote sensing imageries but in a limited manner for sonar imageries, mainly because of the different characteristics of the applications. Detecting the existence and type of small target mines is the objective of change detection applied in sonar images. Thus, compared to a few target pixels, a large number of pixels in the sonar images are made up of environment noise and target-like objects that are difficult to discriminate. Meanwhile, the stationary objects on the seafloor tend to have position error when compared among bi-temporal sonar images taken in t_1 and t_2 , due to the error generated in the data collection process [6]. The other issue is the challenge of analyzing whether a 'change of interest' occurred among all the changed pixels resulting from many underlying factors (i.e., object motions, change of objects azimuth, appearance or disappearance of natural matters and appearance of mine). Hence, in order to suppress the recognition error caused by these difficulties and improve efficiency, this paper proposes a new automated approach based on change detection for mine recognition, and the technique is applied to two sets of actual sidescan sonar images.

The remainder of the paper is organized as following. Section II will introduce the related knowledge of our approach, including the former change detection techniques and sidescan sonar imaging principle. Then, a detailed description of this change detection approach will be presented in Section III, and the results will be shown in Section IV. Section V will conclude the paper.

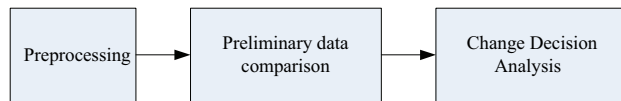


Fig. 1. A system block diagram for change detection

II. RELATED PRINCIPLES

A. Existing Change Detection Techniques

Image change detection is the process of identifying differences in the states of an object or phenomenon by observing multitemporal images taken from the same region at different times [7]. The change detection techniques have been widely used in various applications, such as environmental monitoring [7][10], damage assessment [11], video surveillance [12] and medical diagnosis [13].

A review of bi-temporal change detection techniques [8] reveal that although the change detection methods have many varieties, they share some common processing steps, as summarized in Fig.1.

First, preprocessing is performed to filter out common types of "uninterested" changes caused by sensor geometry, environmental conditions and other factors. Depending on image characteristics, preprocessing can involve a number of alternative steps. For example, registration is required to align bi-temporal images using spatial transformations. Feature matching is required in the case where the regions without objects of interest are stable in the images. Other processes include intensity adjustment, linear transformation of intensity and speckle filter as well.

Then, a comparison of images is performed to find out the differences, or the changes. Here, we call it "preliminary data comparison". The methods for this comparison process are generally regarded as digital change detection algorithms that have been discussed in [7][9][10]. They can be divided into two categories: pixel-level image comparison (such as, image differencing, change vector analysis, image ratioing, and image regression) and feature-level image comparison (such as, post-classification comparison, direct multi-data classification and vegetation index differencing). Pixel-level image comparison, especially image differencing, is a widely used technique for change detection using remote-sensing data, because it is simple, straightforward and easy to interpret the results. But their disadvantages compared to feature-level image comparison are obvious given that they are sensitive to misregistration between two images and cannot provide a detailed change matrix. More importantly, a lot of information may be discarded from the data in the subtraction process. Such subtraction results in the loss of small areas of change. Moreover, the original shape and size of an object are likely to be destroyed which may harm subsequent feature analysis. On the other hand, feature-level image comparison methods can bypass the problem of requiring accurate registration of bi-temporal images and provide more change information for analysis. Nevertheless, the final accuracy of these approaches depends on the quality

of the classified images, and small errors in classification may magnify the overall change detection error.

At last, the decision of whether the changes are relevant to the user is taken. Ideally, the result of this step can be obtained by thresholding after image comparison. But, for sonar images with many clutters, it is challenging to identify the exact threshold for determining whether change happened and what the changes were. Thus, some researchers proposed statistical likelihood tests [8] for change decision analysis, while others regard change decision as a classification problem (change class/no-change class) and adopt machine learning algorithms to address this problem [14].

B. Sidescan Sonar Images

The sidescan sonar imagery is generated by periodically transmitting acoustic pulses orthogonal to the direction of underwater sonar arrays' motion, and receiving the returning echo data recorded by lines [15]. Usually, there are two sonar arrays mounted on the each side of the underwater towfish that transmit the fan-shaped acoustic wave beams vertically from left and right respectively. Then the backscatter signals from the seafloor are received in a temporal sequence and plotted as a two-dimensional image. Due to the strong backscatter from objects, objects in the regions are represented as 'bright-light's in the sonar images, while, acoustic wave beams can not reach the regions behind objects where sonar images show a 'shadow'. Obviously, two-dimensional images can not accurately depict the three-dimensional objects but shadow pixels of objects are two-dimensional that can be observed from the images. Thus, the height and shape of the bottom objects are generally estimated through the characteristics of the shadow (i.e., shape and length) in the sonar image analysis.

In our paper, three sidescan sonar images obtained by a Klein 5500 sidescan sonar in Fig.2 are used, the detailed description of which is provided in [16]. These images cover roughly the same area in the same direction. Among them, one (Fig.2(a)) was taken on *January30th*, 2008, called *History Image (HI)* in this paper, while the other two images were taken on *February18th*, 2008, called *Current Images (CI)* in this paper. These two CIs, i.e., CI1(Fig.2(b)) and CI2(Fig.2(c)), present two types of target mines (labeled with a circle in Fig. 2). CI1 contains a cylinder-like mine, and CI2 contains a cone-like mine. All of them are grey-level scale images with a normal resolution of 0.11m by 0.11m.

III. AUTOMATED CHANGE DETECTION APPROACH USING SIDESCAN SONAR IMAGES

As shown in the flow chart of Fig.1, the proposed approach of automated change detection consists of three steps. Shadow extraction is done in the first step and the subsequent steps involve processing of the shadows, e.g., extraction and classification of shadows. The reason is that, as discussed in the previous section, the shadow provides important and overall information of an object in sonar images. Moreover, man-made objects usually have regular shapes and smooth surfaces, which can generate well-regulated shadow regions. Then, a method

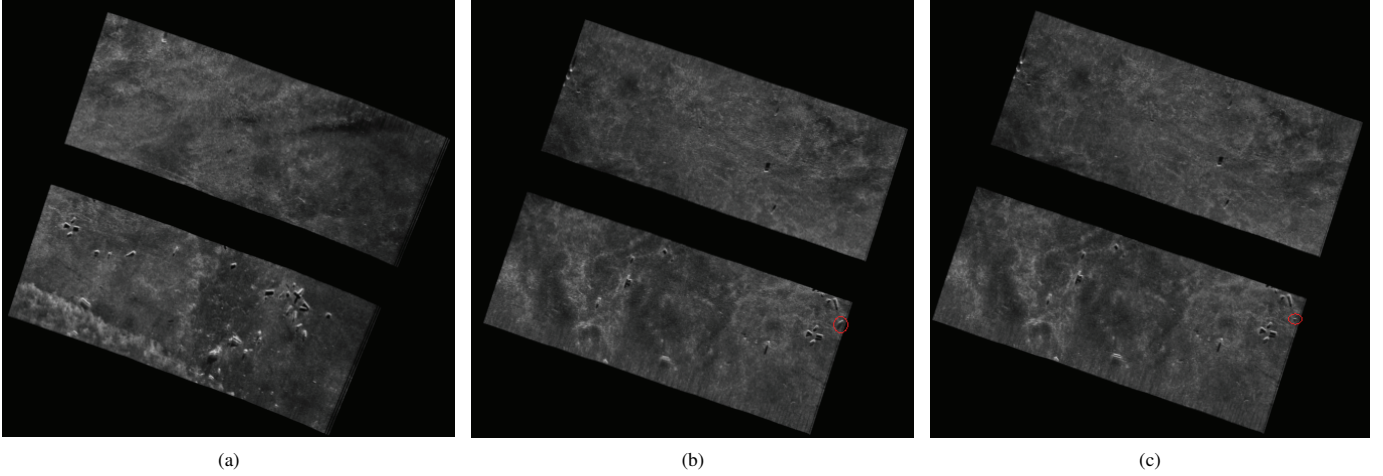


Fig. 2. The original sidescan sonar images: HI (a); CI1 (b); CI2 (c)

based on feature-level image comparison is adopted in our approach. It firstly classifies each object as MLOs or non-MLOs and then generates the change objects by comparing two special features of all the MLOs in bi-temporal images. Finally, a change decision is made among all the change objects using statistical information of the pixels.

A. Preprocessing

Observing the original images in Fig. 2, we found that the backgrounds of the sonar images taken on different dates are not constant. It is caused by the wake of ships crossing the regions of interest and downward refracting environment which presents irregular patterns in the sonar images. Hence, image smoothing and filters are implemented to eliminate the background noise in this step of our approach. Besides, it is worth noting that our approach finally utilizes the 'shape' feature to extract shadow-like snippets separated from other environmental snippets during preprocessing. Considering that the subsequent step based on feature-level image comparison has no requirement for image registration, our approach is designed without registration which can save much workload and reduce the computation complexity.

Since a large amount of "Pepper and Salt Noise" exists in the original sidescan sonar images, as shown in Fig. 2, median filters are first employed to smooth the images and reduce the noise. More specifically, a diamond-shaped median filter with a window size 1 and a 3 by 3 square median filter are sequentially applied to each image (i.e., HI, CI1 and CI2). After image smoothing, the shadow pixels are separated from the background pixels by setting a threshold. All shadow pixels are set to 1 while all the background pixels are set to 0, providing binary images. For each binary image, all the connected pixels are then accumulated as a snippet and all the snippets are labeled. In order to delete those fragmental pixels, the snippets with a tiny size are removed. The results are shown in the Fig. 3.

The last step of preprocessing is to remove the redundant snippets using their "shape" features. The "shape" feature, S , is defined as the proportion of the squared perimeter (P) and the area (A) of a snippet x in the binary images of Fig.3. Mathematically, it is defined as Eq.(1).

$$S(x) = \frac{P(x)^2}{A(x)} \quad (1)$$

The value of the "shape" feature is high if a snippet has many holes and ragged edges. The big difference between the shadow and environmental noise is that the pixels of a shadow are close to each other. Hence, a snippet with a smaller value of the shape feature has a higher possibility to be a shadow than the disturbance reflection from seafloor. Here, the threshold value is defined as 20. The results after removing the redundant snippets are shown in the Fig. 4.

B. Preliminary data comparison

This step chooses post-classification comparison to obtain the candidate changes. MLOs are firstly detected by classification, which is performed by checking the bright-light information in the neighboring regions of each snippet. This is because non-MLOs usually have no bright-light near the shadow or have the bright light at a large distance from the corresponding shadow. A 100 by 100 square window is created to restrict the neighboring regions of every shadow snippet (W) by taking W as the center of the window. Then, bright-light snippets (B) are extracted from every window by defining a threshold. Considering that the objects are so close, the windows may overlap with each other, thus association between W and B is done by mating W and B with the smallest Euclidean distance between their center pixels. The classification result is then determined by analyzing the B - W pairs using the following rule.

- 1) For all the W , assuming the partner of a W_i is B_j , if they are enclosed in the same window, i.e., their

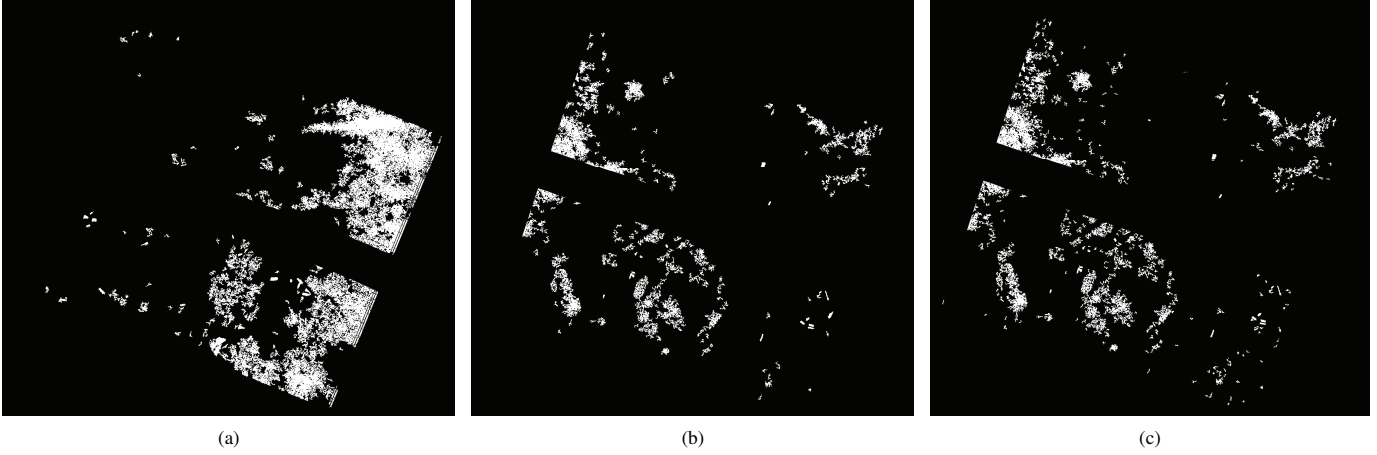


Fig. 3. The shadow results after image smoothing and removing the tiny snippets in HI (a), CI1 (b) and CI2 (c)

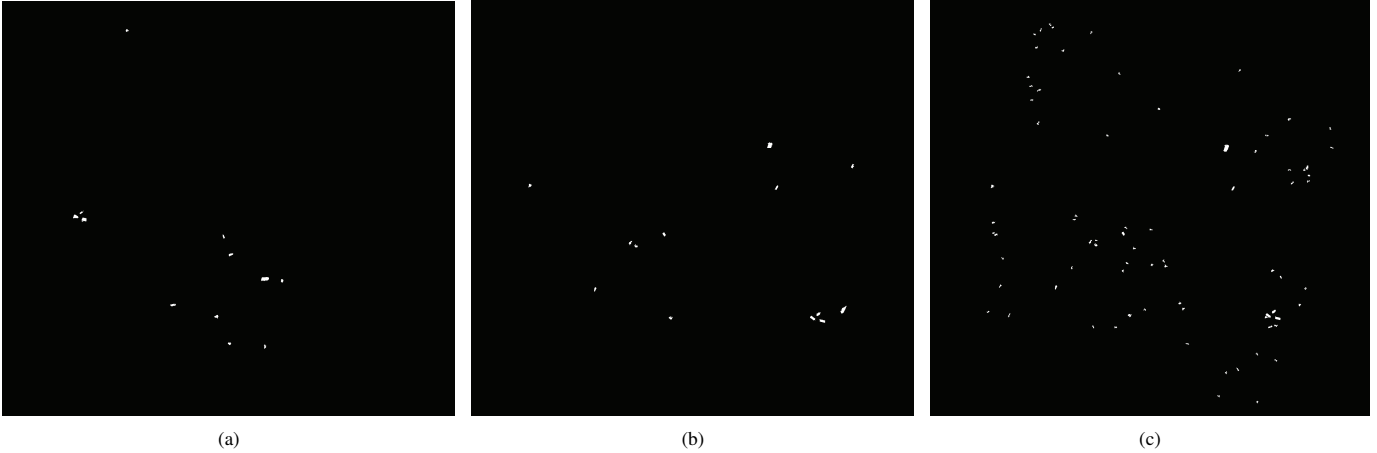


Fig. 4. The shadow results after preprocessing in HI (a), CI1 (b) and CI2 (c)

distance between the center pixels should be smaller than 100, then B_j is classified as the bright light of MLOs ($MLOs - B_j$);

- 2) For all the $MLOs - B$, if W_k is located at the nearest place of a $MLOs - B_j$, W_k is classified as the shadow of MLOs ($MLOs - W_k$).

As a result, 7 MLOs were found in HI, 7 MLOs in CI1 and 13 MLOs in CI2.

After classification, an analysis of geometry location and coarseness of each of the $MLOs - W$ is performed for change detection. If a $MLOs - W$ in CI (CI1 or CI2) is in the same geometry location as in HI or within an allowable error range, we consider it as "no change". Sometimes, a few objects are close-by in terms of geometry location, such as, a "constellation" of targets in our data. Furthermore, it is also possible that different objects appear at the same location but at different times. Hence, using geometry location is not enough. Another feature, "coarseness", a kind of texture features based

on visual perception, is introduced in this study. Selecting coarseness is useful because man-made mine objects have a more regular shape of shadows than clutters, as illustrated in Fig. 5. In addition, coarseness of an object provides the important internal characteristics of texture construction which is constant at different times for every part of the surface of an object, so that it is not sensitive to the change of object size and position azimuth. Here, Tamura textural features are employed to compute the coarseness of an object. The coarseness and its calculation is given below.

- 1) For every pixel $p(x, y)$ at the (x, y) position of a image presented a $MLOs - W$, assume a moving window with the size of 2^k by 2^k pixels and compute its average intensity $A_k(x, y)$ around the pixel using Eq.(2). (k is initially defined as 0)

$$A_k(x, y) = \sum_{i=x-2^{k-1}}^{x+2^{k-1}-1} \sum_{j=y-2^{k-1}}^{y+2^{k-1}-1} \frac{p(i, j)}{2^{2k}}; \quad (2)$$

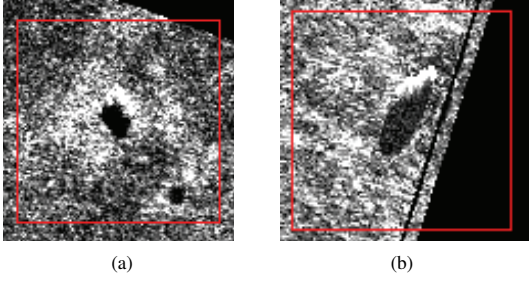


Fig. 5. One clutter (a) and the cylinder target (b) in the sonar images

- 2) For every pixel $p(x, y)$, calculate the absolute difference $E_k(x, y)$ between the average intensities of the non-overlapping window-pairs in the horizontal ($E_{k,h}(x, y)$) and vertical ($E_{k,v}(x, y)$) directions, as Eq.(3).

$$\begin{aligned} E_{k,h}(x, y) & \\ = |A_k(x + 2^{k-1}, y) - A_k(x - 2^{k-1}, y)|; & \\ E_{k,v}(x, y) & \\ = |A_k(x, y + 2^{k-1}) - A_k(x, y - 2^{k-1})|; & \end{aligned} \quad (3)$$

- 3) Repeat the step 1-2 by setting k from 0 to n and find the value of $k_{best(x,y)}$ that maximizes the difference in either direction for every (x, y) . The value of n depends on the size of the image as long as four times of any moving window are not larger than the entire image, then its maximum is 5.
- 4) Finally, the coarseness value of an image $F_{coarseness}$ with the size of m by n pixels is obtained by averaging the areas of all the best windows for every pixel (x, y) as Eq.(4).

$$F_{coarseness} = \frac{1}{m * n} \sum_{i=1}^m \sum_{j=1}^n 2^{k_{best(i,j)}}; \quad (4)$$

By comparing the MLOs-W in HI and CI using the geometry location and the coarseness, the changes in CI from HI can be identified. Fig. 6 shows the identified changes in CI1 and CI2, respectively. One example is that the "constellation" that is in the same place at different times is removed after comparison.

C. Change decision analysis

Finally, our approach makes the change decision according to the pixel distribution of each change. The reason is that the target which is a man-made object has a normal-like pixel distribution while the pixel distribution of other natural objects in the seafloor is irregular. Fig. 7 shows a comparison figure of pixel distributions of some clutters and the targets of interest. Subsequently, this approach calculates the mean squared error (MSE) between the real pixel distribution of each object and its

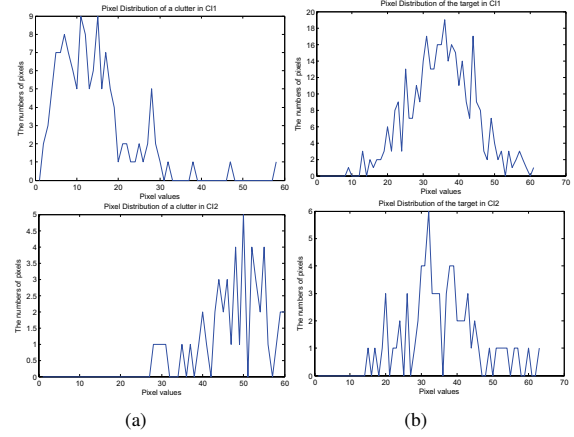


Fig. 7. One clutter (a) and the cylinder target (b) in the sonar images

TABLE I
RESULTS FOR CHANGE DETECTION OF CI1 AND CI2

Results	Image CI1	Image CI2
Target detected	1/1	1/1
Change detected	2	5
False alarms (numbers of objects)	1	4
False alarms (percentage of pixels)	0.0026%	0.0073%

corresponding ideal Gaussian distribution function, as Eq.(5).

$$\begin{aligned} F_{distribution}(I) &= \\ \frac{\sum_{i=1}^{pn} (D(i) - D(\frac{1+pn}{2})) * exp(-\frac{(i - \frac{1+pn}{2})^2}{\sigma^2})^2}{pn} & \end{aligned} \quad (5)$$

where pn denotes the total numbers of pixel values in a changed object's image I and $D(i)$ means the distribution of the pixel value as i . The parameters of the ideal Gaussian function are obtained by satisfying an arbitrary non-zero point of the pixel distribution curve of I . If the value of $F_{distribution}(I)$ is within $[0, 1]$, the corresponding object of the image I is considered as the target of interest. Otherwise, it is said to be clutter. Using this method, it was found that the two targets of interest in CI1 and CI2 can be detected. The false alarms associated with detecting these two targets of interest, presented by percentage of pixels, are 0.0026% and 0.0073%, respectively. Table I shows the results in detail, including the number of targets detected out of the actual number of targets, the changed objects detected and the false alarms represented by the number of objects and percentage of pixels respectively. It can be seen that this approach is capable of recognizing the mine targets correctly with fewer false alarms.

IV. CONCLUSION

An automated method based on change detection techniques for mine recognition using sidescan sonar images is proposed in this paper, and it has been successfully applied in a real dataset. Unlike the existing methods for the MDC problem



(a)



(b)

Fig. 6. Results after preliminary data comparison of HI and CI1 (a); HI and CI2 (b)

that demand extensive training data or aprior information about the application, our approach employed change detection techniques to solve the problem by only analyzing the change between the sidescan sonar images on two different dates that can be easily collected using route survey operations. In this approach, image smoothing and "shape" feature extraction of snippets are preprocessed to suppress the background noise and variation due to ship wakes or refracting environment, and shadows of interest are extracted for analysis. Then, post-classification comparison is applied to detect the MLOs and classify the changed objects using the relationship between bright-lights and the corresponding shadows and the stable coarseness character of an object. At last, the final change decision is obtained by analyzing the statistical information of the pixel distribution of classified changes, since a man-made object generally has regular shapes and smooth surfaces, their pixel distributions are similar to a normal distribution. After applying to two sets of real data, the image results and false alarms are presented in this paper, which can verify the ability of our proposed approach to address the MDC problem. In the future, we would like to improve the theoretical model of our approach and apply it to analyze other sonar images with different situations.

REFERENCES

- [1] G. J. Dobeck, J. C. Hyland and L. Smedley, "Automated detection/classification of sea mines in sonar imagery", *Proc. SPIE-Int. Soc. Optics*, vol. 3079, pp. 90-110, 1997.
- [2] C. M. Ciany and W. Zurawski, "Performance of computer aided Detection/Computer Aided Classification and data fusion algorithms for automated detection and classification of underwater mines", in *Proc. CAD/CAC Conf.*, Halifax, NS, Canada, Nov. 2001.
- [3] T. Aridgides, M. Frenandez and G. Dobeck, "Fusion of adaptive algorithms for the classification of sea mines using high resolution side scan sonar in very shallow water", in *Proc. MTE/IEEE Oceans Conf. and Exhibition*, vol. 1, pp. 135-142, 2001.
- [4] S. Reed, Y. Petillot, and J. Bell, "An automatic approach to the detection and extraction of mine features in sidescan sonar", *IEEE journal of oceanic engineering*, Vol. 28, No. 1, Jan. 2003.
- [5] S. Reed, Y. Petillot and J. Bell, "Automated approach to classification of mine-like objects in sidescan sonar using highlight and shadow information", In *Proc. Radar, Sonar and Navigation*, Volume 151, Issue 1, Feb 2004.
- [6] M. L. Gendron and M. C. Lohrenz, "The automated change detection and classification real-time (ACDC-RT) system", In *Proc. Oceans 2007-Europe*, pp. 1-4, June 2007.
- [7] A. Singh, "Review Article: Digital change detection techniques using remotely-sensed data", *Int. J. Remote Sens.*, vol. 10, no. 6, pp. 989-1003, 1989.
- [8] Richard J. Radke, Srinivas Andra, Omar Al-Kofahi and Badrinath Roysam, "Image change detection algorithms: a systematic survey", *IEEE Transactions on Image Processing*, vol. 14, no. 3, March 2005.
- [9] D. Lu, P. Mausel, E. Brondizo and E. Moran, "Change detection techniques", *Int. J. Remote Sens.*, vol. 25, no.12, pp. 2365-2407, 2003.
- [10] P. Coppin, I. Jonckheere, K. Nackaerts and B. Muys, "Digital change detection methods in ecosystem monitoring: a review", *Int. J. Remote Sens.*, vol. 25, no. 9, pp. 1565-1596, May, 2004.
- [11] F. Bovolo, L. Bruzzone, "A splite-based approach to unsupervised change detection in large-size multitemporal image: application to Tsunami-Damage assessment", *IEEE Trans. on Geosci. Remote Sensing*, vol. 45, no. 6, June 2007.
- [12] Mark J. Carlotto, "A Cluster-Based Approach for Detecting Man-Made Objects and Changes in Imagery", *IEEE Transaction on Geosci. Remote Sensing*, vol. 43, no. 2, Feb. 2005.
- [13] Harihar Narasimha-Iyer, Ali Can, Badrinath Roysam, Charles V. Stewart, Howard L. Tanenbaum, Anna Majerovics, and Hanumant Singh, "Robust detection and classification of longitudinal changes in color retinal fundus images for monitoring diabetic retinopathy", *IEEE Transaction on Biomedical Engineering*, vol. 53, no. 6, June 2006.
- [14] F. Bovolo, L. Bruzzone and M. Marconcini, "A novel approach to unsupervised change detection based on a semisupervised SVM and a similarity measure", *IEEE Transaction on Geosci. Remote Sensing*, vol. 46, no. 7, July 2008.
- [15] S. G. Johnson and M. A. Deaett, "The application of automated recognition techniques to side-scan sonar imagery", *IEEE Journal of Oceanic Engineering*, vol. 19, no. 1, Jan. 1994.
- [16] Myers, V., "A data set for change detection in port environments using sidescan sonar," *DRDC Atlantic Tech. Mem. TM2008-247*, 2008.